

Load Frequency Control of Two-Area Thermal Power System with HVDC-SMES unit Under Different Inertia Strategies using PSO

I. Kameswari, G.Pavan Kumar

Abstract: The paper is copied with stability enhancement of power system by precise method for designing, simulation and better adjustment of the parameters of the secondary control with HVDC link and SMES unit are presented. PSO is employed to search for better controlling parameters and the arrangement for the suggested controller is defined as an optimum issue. For the system's better performance the different inertia weight strategies in PSO are also applied. The complete study of choosing the objective function and controller design on the efficiency of the HVDC link and SMES unit is done and given the simulated results. Dynamic response of the power structure is increased when inserted HVDC link along with SMES unit. Adopting SIMULINK/MATLAB environment the results are simulated.

Index Terms: ACE, HVDC link, LFC, PID controller, PSO and SMES unit.

I. INTRODUCTION

The utility power system main objective is to provide consumers a less cost and continuous power by balancing the power generation and power demand. As the system is a huge and complex electrical unit consisting of generating, transmitting and distributing units with loads that shared over large area through the entire network [1]. Due to the sudden load changes the power flow in tie-line and system frequency is affected by active power load and to bear the nominal values of both the power flow in tie-line and system frequency interchange value for the primary regulation loop of ALFC or AGC is used. In practical interconnected system's it is not an easy task to keep the frequency at a fixed point due to various uncertainties available due to demand fluctuations [2, 4]. To sustain the tie-line power and system frequency at their rated values during random load disturbances and during usual operating conditions, several control techniques are suggested for AGC systems [3]. Whatever the control method adopted, the main aim is to calculate the gains of respective PID controller which keep the power in tie-line inside the bounds and to keep the frequency of every area inside the predefined limits by satisfying the system constraints and reduce the uncertainties [5].

Revised Manuscript Received on June 01, 2019.

I.Kameswari, Department of Electrical & Electronics Engineering, SRKR Engineering College, Bhimavaram, Andhra Pradesh, India, ilurikameswari@gmail.com.

G.Pavan Kumar, Department of Electrical & Electronics Engineering, SRKR Engineering College, Bhimavaram, Andhra Pradesh, India, gpavan16@gmail.com.

To adjust the PID controller gain constants for fulfilling the system requirements the PSO is commonly employed. The LFC problem is very significant zone in the integrated power grid. L.K.Kirchmayer and C.concordia have performed a major portion of work on LFC in the literature survey. Admirable efforts on LFC grid is proposed by O.I.Elgerd [6]. Power structure is non-linear network which is complex in nature and encountered with various circumstances. Even with several fluctuations in demand of the power supply, Frequency should be kept constant for reliability of supply. For LFC, several control techniques are presented now-a-days. GA is adaptive and powerful method to determine search and optimization issue but its complication of organizing made it hard for execution and also its merging acceleration [7].

BFOA [8] is a strategy which maintains the frequency inside the tolerable range by adjusting the gains of controller and handle with propagation procedure and initiate more parameters to be varied with N individuals of the population which is a drawback of it which leads to another technique that is PSO which is based on the population first discussed by Russell C.Eberhart and James Kennedy in 1995 [9]. LFC of two area coordinated system is performed by adjusting the PID controllers by meta-heuristic optimizing techniques. Going through literary survey it is clear that PSO is better method. Dynamic response of power structure is improved by connecting HVDC link [10] in parallel with the AC tie-line. HVDC controls the power in tie-line by altering the angle of conduction at converter stations. Speed damping phenomena can be increased by providing SMES unit [11] which is an energy storage device which increase effective response of the system by releasing the stored energy to the system through the converter at the time of abrupt rise in load requirement [12]. For better operation of the system the error objective is obtained by considering power in tie-line and variation in frequency of control regions called Area Control Error (ACE). Main target of this work is to reduce the ACE by PSO.



II. SYSTEM STUDIED

Interconnected two-area with non-reheat type thermal power structure with PID controller in two unequal areas named as area-one and area-two is studied. For preparing the structure feasible, time constraints and parameters of various values are to be considered for area-one and area-two. Every area has a central facility to monitor power in tie-line and system frequency called the energy control center. It is concealed that there is step load interruption in the control area-one. The linear comboof power variation in tie-line and error in frequency called as ACE. Theinput for secondary controllers are given from ACE's. U_1 and U_2 are the outputs of the secondary controllers are. Fig.1 shows the ACE's as follows:

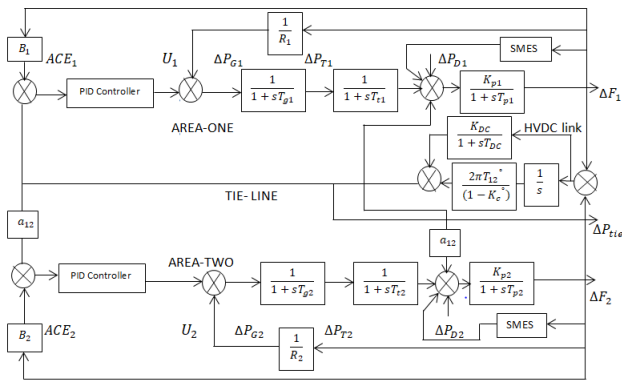


Fig.1. Transfer function model of two-area system

Where ΔP_{12} and ΔP_{21} are the tie-line power changes in area-one and area-two. When the structure is projected for small variation, the ACE's are considered as activating signals for reducing ΔP_{tie} and ΔF to zero when the normal condition is attained. For increasing transient response of the structure, input and output scaling factors of the secondary controller should be perfectly chosen.

III. TIE-LINE AND HVDC LINK TRANSFER FUNCTION MODELS

Fig.1 shows the LFC system interconnected with HVDC and AC tie-line. The HVDC and AC links transfer function models used in LFC studies are described below:

A. Tie-line

The below equation describes the tie-line transfer function model:

$$\Delta P_{tieAC}(s) = \frac{2\pi T_{12}}{s} (\Delta F_1(s) - \Delta F_2(s)) \quad (1)$$

Where, $T_{12} = \frac{P_{max}}{P_r} \cos(\delta_1^0 - \delta_2^0)$ which indicates tie-line torque synchronization coefficient.

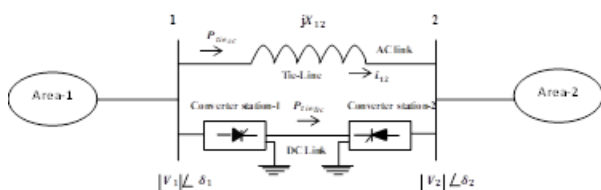


Fig.2 System with two-area interconnection

B. HVDC Link

It is denoted by first order transfer function as shown below:

$$\Delta P_{tieDC}(s) = \frac{K_{DC}}{1+sT_{DC}} \quad (2)$$

Where, T_{DC} is the required time to establish the DC current after load change has occurred in the interconnected areas and K_{DC} is the gain constant of HVDC link.

C. SMES Unit

Transfer function of SMES is as follows:



Fig.3 SMES unit model

SMES control action is elucidated as [5, 11, 12]

$$\Delta E_d = \frac{1}{1+sT_{dc}} [K_{SMES} (B_i \Delta \omega_i + \Delta P_{ij}) - K_{id} \Delta I_{di}] \quad (3)$$

IV. OPTIMIZATION OF PID CONTROLLER GAIN SETTINGS

LFC objective function is to reduce the value of ACE to zero. For attaining this, the two areas cost objective f is considered as the integral square error (ISE) of the radian frequency (ω):

$$ISE = \int_0^{t_s} (\Delta F_1^2 + \Delta F_2^2 + \Delta P_{tie}^2) dt \quad (4)$$

Where, ΔF_1 and ΔF_2 are the change in frequencies in area-one and area-two commonly. ΔP_{tie} is the tie-line power change.

Minimize f, subjected to $K_{Pmin} \leq K_P \leq K_{Pmax}$; $K_{Imin} \leq K_I \leq K_{Imax}$; $K_{Dmin} \leq K_D \leq K_{Dmax}$.

Where, K_{Pmax} , K_{Imax} , K_{Dmax} and K_{Pmin} , K_{Imin} , K_{Dmin} are maximum and minimum control parameter values.

V. PSO ALGORITHM

PSO is commenced by R.C.Eberhart and James Kennedy in 1995 [9]. Particle swarm methodology optimizes non-linear functions, based on flocking of birds technique. Inertia weight contributes balance and plays a major role and decides the rate of contribution of the current step velocity and particle's previous velocity. The different inertia weight strategies are suggested by P. K. Singh, M.Saraswat and J.C.Bansal [13]. Experimentally best results can be obtained with inertia weight ranging between 0.4 to 0.9. Set the control parameters of the PSO. Generate randomly velocities (v) and positions (x) of particle. By updating the velocities and positions by the following equations 5,6,7,8 obtain the fitness function of various particles by comparing the global best to local best of each population until the desired fitness is reached. Based on the performance index minimum value of PID controller is tuned.

For i^{th} particle position and velocity are generated as follows:

$$X_o^i = X_{min} + (X_{max} - X_{min}) \times rand \quad (5)$$

$$V_o^i = V_{min} + (V_{max} - V_{min}) \times rand \quad (6)$$

The velocity of i^{th} particle is updated as, $V_{k+1}^i = V_k^i + C_1 * rand (P_{bestk}^i - X_k^i) + C_2 * rand (G_{best}^i - X_k^i)$ (7)

The position of the particle is updated as



$$X_{k+1}^i = X_k^i + V_{k+1}^i \quad (8)$$

VI. RESULTS

In this part, behavior of the system with two areas interconnected under step load variation of 10% in area-one is examined. PID controller parameters are tuned using the PSO algorithm. To analyze the system for five inertia weight strategies in the PSO algorithm for balancing the examination and bleeding procedure of flock as it has effect of initial velocity and inertia weight (w) is considered for controlling particles velocity. For comparing different methods to set best inertia weight for the better dynamic response of the system, inertia weight for PSO is considered in the paper and analysis is done by implementing different inertia weight strategies for LFC issue. The simulation results are shown in the below figures. Here, for each case the simulation results are compared by evaluating the system:

- With secondary control
- With secondary control and HVDC link
- With secondary control, HVDC link and SMES unit

A. Constant Inertia weight

The dynamic response of frequency change in area-one for load change of 10% in it with secondary control; secondary control and HVDC link and with secondary control, HVDC link and SMES unit for the constant inertia weight as in Fig.4.

Dynamic performance of frequency variation in area-two for 10% step change in area-one with secondary control; secondary control and HVDC link; and with secondary control, HVDC link and SMES unit for the constant inertia weight as shown in Fig.5.

The dynamic response of power variation in tie-line for 10% step change in area-one with secondary control; secondary control and HVDC link; and with secondary control, HVDC link and SMES unit for the constant inertia weight as shown in Fig.6.

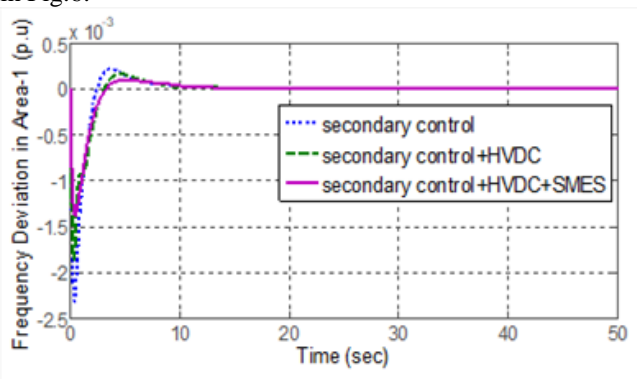


Fig.4 Variation of frequency in area-one for 10% change in load in area-one

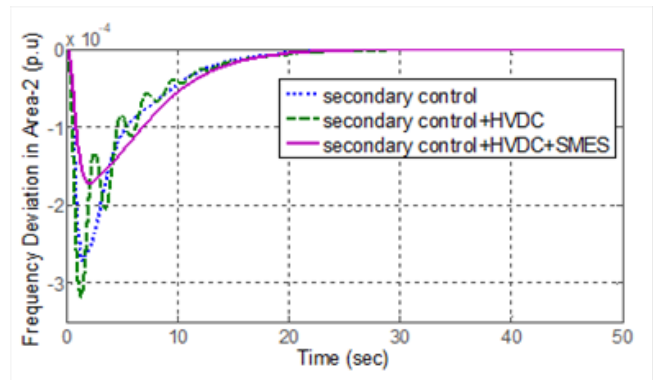


Fig.5 Variation in frequency in area-two for 10% change in load in area-one

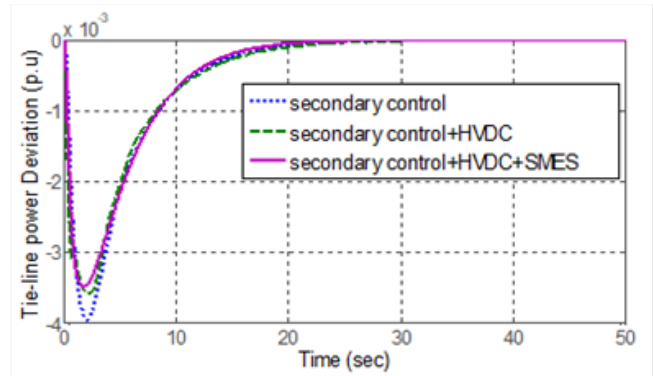


Fig.6 Variation in power in tie-line for change of 10% in load in area-one

B. Random Inertia Weight

The dynamic response of frequency change in area-one for step change of 10% in it with secondary control; secondary control and HVDC link; and with secondary control, HVDC link and SMES unit for the random inertia weight as in Fig.7. Dynamic response of variation of frequency in area-two for 10% step change in area-one with secondary control; secondary control and HVDC link; and with secondary control, HVDC link and SMES unit for the random inertia weight as shown in Fig.8.

The dynamic response of variation in tie-line power for step load change of 10% in area-one with secondary control; secondary control and HVDC link; and with secondary control, HVDC link and SMES unit for the random inertia weight as in Fig.9.

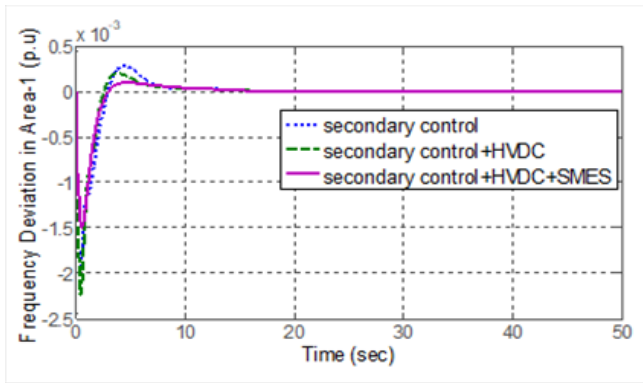


Fig.7 Variation of frequency in area-one for change in load of 10% in area-one

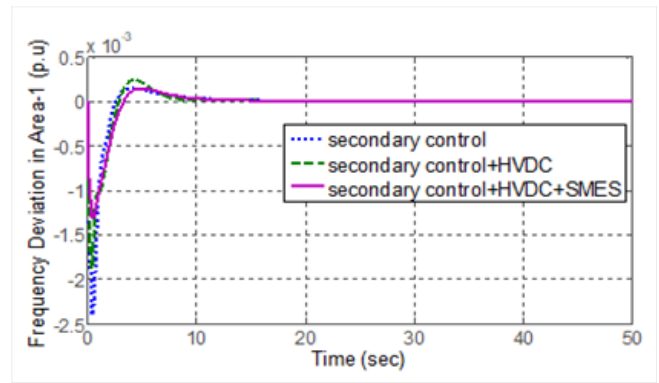


Fig.10 Variation of frequency in area-one for change in load of 10% in area-1

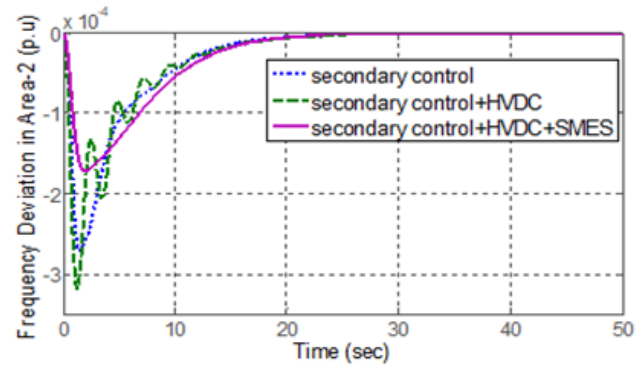


Fig.8 Variation of frequency in area-two for change in load of 10% in area-one

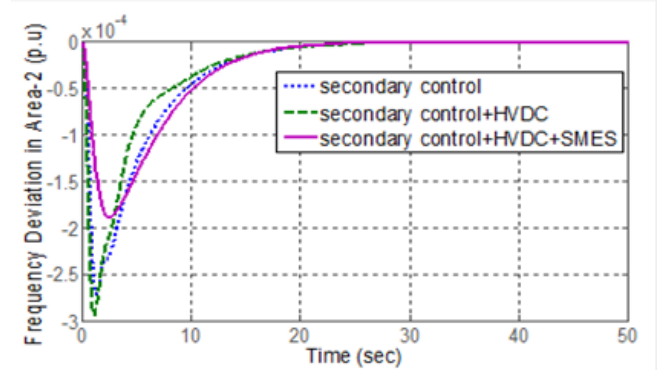


Fig.11 Variation of frequency in area-two for change in load of 10% in area-one

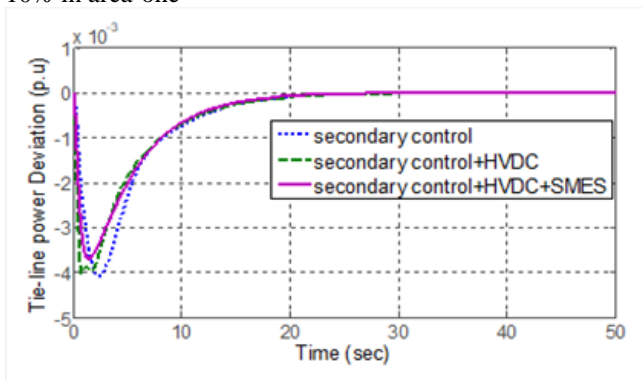


Fig.9 Tie-line power variation for change in load of 10% in area-one

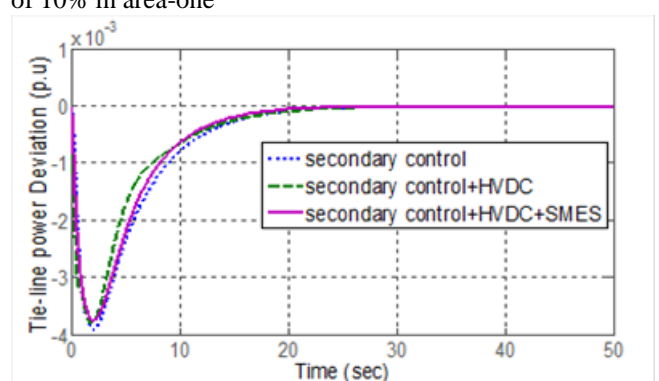


Fig.12 Tie-line power variation for change in load of 10% in area-one

C. Linear Decreasing Inertia Weight

Dynamic performance of frequency variation in area-one for change in load of 10% in it with secondary control; secondary control and HVDC link; and with secondary control, HVDC link and SMES unit for the linear decreasing inertia weight as in Fig.10.

Dynamic performance of variation of frequency in area-two for 10% change in load in area-one with secondary control; secondary control and HVDC link; and with secondary control, HVDC link and SMES unit as in Fig.11 for the linear decreasing inertia weight.

Dynamic response of change in power flow in tie-line for change in load of 10% in area-one with secondary control; secondary control and HVDC link; and with secondary control, HVDC link and SMES unit for the linear decreasing inertia weight as in Fig.12.

D. Global Best Inertia Weight

Dynamic response of frequency change in area-one for step change of 10% in it with secondary control; secondary control and HVDC link; and with secondary control, HVDC link and SMES unit as in Fig.13.

Dynamic performance of frequency variation in area-two for 10% step change in area-one with secondary control; secondary control and HVDC link; and with secondary control, HVDC link and SMES unit for the global best inertia weight as shown in Fig.14.

The dynamic response of tie-line power flow variation for change in load of 10% in area-one with secondary control; secondary control and HVDC link; and with secondary control, HVDC link and SMES unit for the global best inertia weight as in Fig.15.

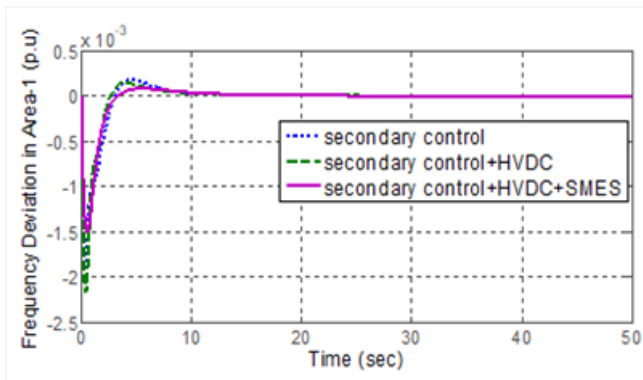


Fig.13 Variation in frequency in area-one for change in load of 10% in area-one

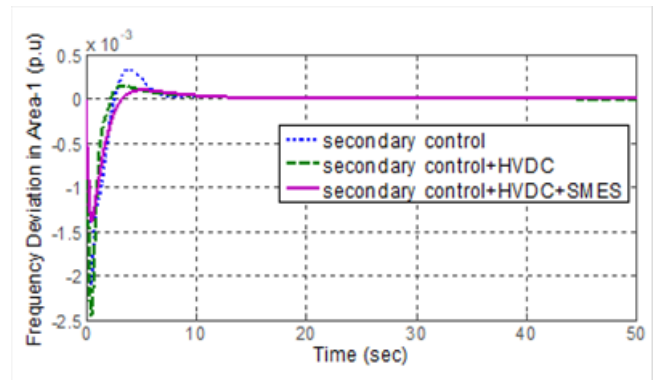


Fig.16 Variation of frequency in area-one for 10% change in load in area-one

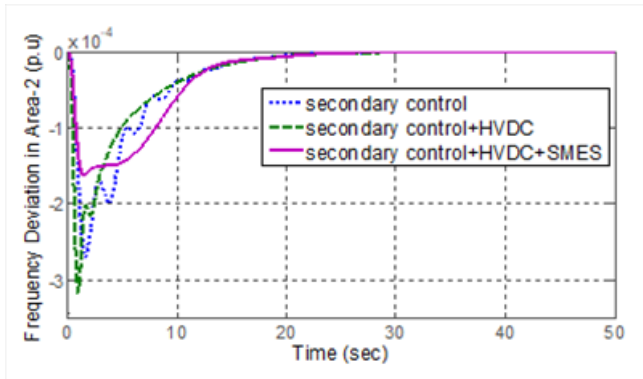


Fig.14 Change in frequency in area-two for change in load of 10% in area-one

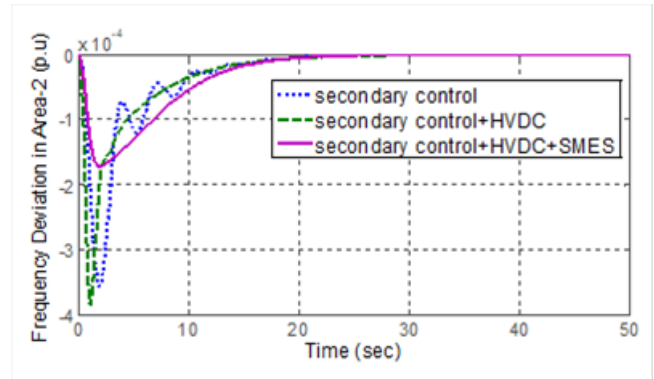


Fig.17 variation of frequency in area-one for change in load of 10% in area-one

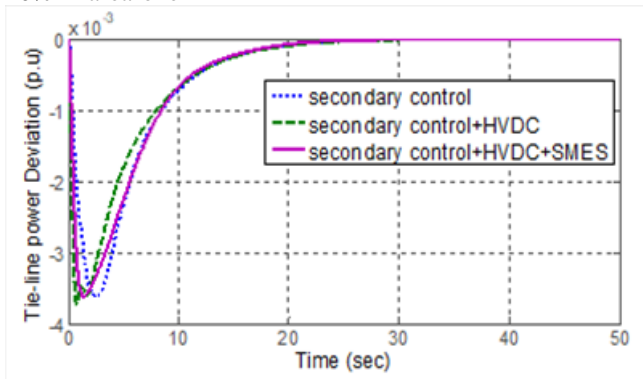


Fig.15 Variation of tie-line power flow for load change of 10% in area-one

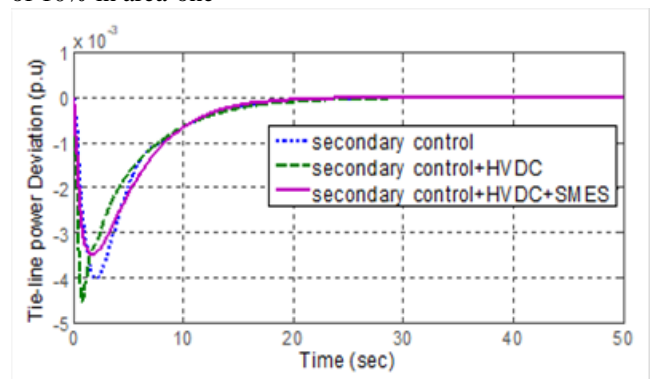


Fig.18 Variation of power flow in tie-line for 10% load change in area-one

E. Simulated Annealing Inertia Weight

The dynamic response of frequency change in area-one for load change of 10% in it with secondary control; secondary control and HVDC link; and with secondary control, HVDC link and SMES unit for the simulated annealing inertia weight as in Fig.16.

Dynamic performance of variation of frequency in area-two for load change of 10% in area-one with secondary control; secondary control and HVDC link; and with secondary control, HVDC link and SMES unit for the simulated annealing inertia weight as in Fig.17.

Dynamic response of deviation in power flow in tie-line for load change of 10% in area-one with secondary control; secondary control and HVDC link; and with secondary control, HVDC link and SMES unit for the simulated annealing inertia weight as in Fig.18.

F. Comparison of different inertia methods

Dynamic performances of frequency changes in the two areas and deviation of power flow of tie-line for load change of 10% in area-one when SMES is connected to the system along the HVDC link are as follows:

Dynamic response of frequency change in area-one for 10% load disturbance in area-one with SMES unit connected for the five different inertia methods as in Fig.19.

Dynamic response of frequency change in area-two for 10% load disturbance in area-one with SMES unit connected for the five different inertia methods as in Fig.20.

Dynamic response of change in power flow in tie-line for stepchange of 10% in area-one for the five inertia weight strategies with SMES unit connected as in Fig.21.

Load Frequency Control of Two-Area Thermal Power System with HVDC-SMES unit Under Different Inertia Strategies using PSO

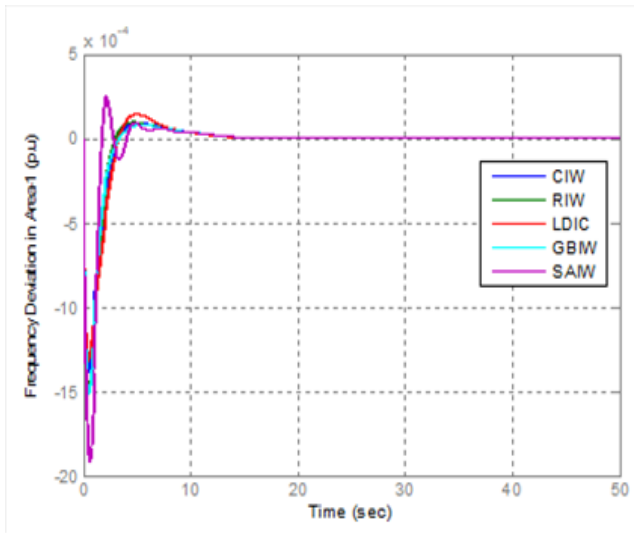


Fig.19 Variation of frequency in area-one for load change of 10% in area-one

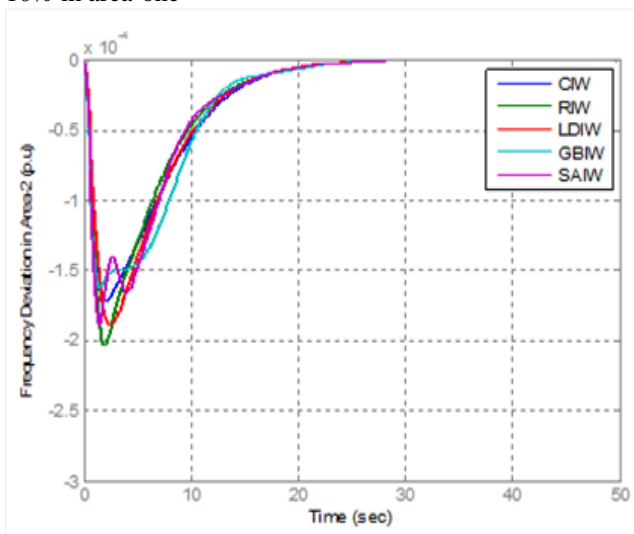


Fig.20 Variation of frequency in area-two for load change of 10% in area-one

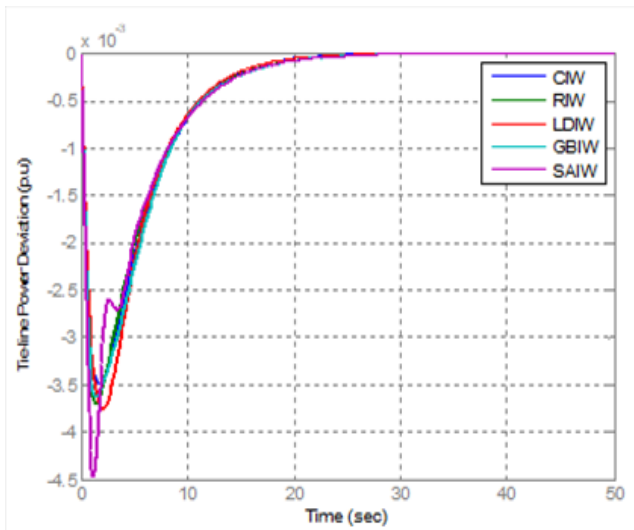


Fig.21 Variation of power flow in tie-line for load change of 10% in area-one

Table-1: Constant Inertia Weight

Different controller strategies		Secondary controller	Secondary with HVDC link	Secondary with HVDC and SMES unit
ΔF_1	peak $\times 10^{-3}$	-2.25	-1.82	-1.37
	t_s	14	15	15
	e_{ss}	0	0	0
ΔF_2	peak $\times 10^{-4}$	-2.55	-2.95	-1.7
	t_s	23	25	24
	e_{ss}	0	0	0
ΔP_{tie}	peak $\times 10^{-3}$	-3.87	-3.55	-3.44
	t_s	24	25	25
	e_{ss}	0	0	0
Min ISE		0.0028	0.0025	0.0025

Table-1 describes the peak value, settling time, steady state error and min ISE of frequency change in the two areas and also the change in power flow in tie-line for the constant inertia weight.

Table-2: Random Inertia Weight

Different controller strategies		Secondary controller	Secondary with HVDC link	Secondary with HVDC and SMES unit
ΔF_1	peak $\times 10^{-3}$	-1.91	-2.17	-1.48
	t_s	14	13	15
	e_{ss}	0	0	0
ΔF_2	peak $\times 10^{-4}$	-3.06	-3.32	-2
	t_s	24	23	23
	e_{ss}	0	0	0
ΔP_{tie}	peak $\times 10^{-3}$	-4	-3.8	-3.65
	t_s	24	24	24
	e_{ss}	0	0	0
Min ISE		0.0030	0.0028	0.0025

Table-2 describes the peak value, settling time, steady state error and min ISE of frequency change in the two areas and also the change in power flow in tie-line for the random inertia weight.

Table-3: Linear Decreasing Inertia Weight

Different controller strategies		Secondary controller	Secondary with HVDC link	Secondary with HVDC and SMES unit
ΔF_1	peak $\times 10^{-3}$	-3.58	-1.84	-1.3
	t_s	15	13	15
	e_{ss}	0	0	0
ΔF_2	peak $\times 10^{-4}$	-3.97	-2.75	-1.87
	t_s	25	24	23
	e_{ss}	0	0	0
ΔP_{tie}	peak $\times 10^{-3}$	-5.8	-3.68	-3.72
	t_s	24	24	24
	e_{ss}	0	0	0
Min ISE		0.0030	0.0025	0.0027

Table-3 describes the peak value, settling time, steady state error and min ISE of frequency change in the two areas and also the change in power flow in tie-line for the linear decreasing inertia weight.

Table-4: Global Best Inertia Weight

Different controller strategies		Secondary controller	Secondary with HVDC link	Secondary with HVDC and SMES unit
ΔF_1	peak $\times 10^{-3}$	-1.85	-2.1	-1.5
	t_s	14	13	16
	e_{ss}	0	0	0
ΔF_2	peak $\times 10^{-4}$	-2.54	-3.12	-1.6
	t_s	23	24	25
	e_{ss}	0	0	0
ΔP_{tie}	peak $\times 10^{-3}$	-3.6	-3.54	-3.58
	t_s	24	25	25
	e_{ss}	0	0	0
Min ISE		0.0026	0.0024	0.0027

Table-4 describes the peak value, settling time, steady state error and min ISE of frequency change in the two areas and also the change in power flow in tie-line for the global best inertia weight.

Table-5 describes the peak value, settling time, steady state error and min ISE of frequency change in the two areas and also the change in power flow in tie-line for the simulated annealing inertia weight.

Table-6 describes the peak value and min ISE of the change in frequency in two areas for different inertia strategies.

Table-5: Simulated Annealing Inertia Weight

Different controller strategies		Secondary controller	Secondary with HVDC link	Secondary with HVDC and SMES unit
ΔF_1	peak $\times 10^{-3}$	-2.04	-2.4	-1.9
	t_s	13	13	14
	e_{ss}	0	0	0
ΔF_2	peak $\times 10^{-4}$	-3.4	-3.75	-1.89
	t_s	23	22	23
	e_{ss}	0	0	0
ΔP_{tie}	peak $\times 10^{-3}$	-3.9	-4.32	-4.46
	t_s	23	24	24
	e_{ss}	0	0	0
Min ISE		0.0027	0.0025	0.0026

Table-6: Comparison of different strategies of PSO with SMES units connected in the system

S.No:	Dynamic response	First peak of $\Delta f_1 \times 10^{-3}$	First peak of $\Delta f_2 \times 10^{-4}$	Min ISE
1	CIW	-1.37	-1.7	0.0025
2	RIW	-1.48	-2	0.0025
3	LDIW	-1.3	-1.87	0.0027
4	GBIW	-1.5	-1.6	0.0027
5	SAIW	-1.9	-1.89	0.0026

VII. CONCLUSIONS

This work is done by incorporating SMES units in both unequal areas which are connected to each other in a thermal power system. PSO with different inertia methods are applied to the problem of LFC for adjusting secondary controller. Dynamic performance of two area structure is enhanced by adding a HVDC link parallel to tie-line and also by connecting SMES units in the two areas. Dynamic response of the considered structure is investigated under step load disturbance of 10% in area-1 with PID controller; with PID controller and HVDC link; and with PID controller, HVDC link-SMES unit. The system with secondary controller, HVDC link and SMES unit gives better dynamic performance for every inertia weight strategy in terms of settling time, first peak of oscillation and minimum objective. When compared to inertia methods, linear decreasing inertia weight gives the better dynamic response.

APPENDIX

Values for the considered system as shown below [8, 14, 15]:
 $F=60$ Hz; $T_{12}=0.545$ p.u.; $a_{12}=-1$; $B_1=B_2=0.425$ p.u MW/Hz;
 $T_{PS1}=T_{PS2}=20$ s; $K_{DC}=1$; $T_{DC}=0.2$; $R_1=R_2=2.4$ Hz/p.u;
 $T_{G1}=T_{G2}=0.08$ s; $T_{T1}=T_{T2}=0.3$ s; $K_{PS1}=K_{PS2}=120$ Hz/p.u.



REFERENCES

1. Elgerd OI. Electric energy systems theory. An introduction. 2nd ed. New Delhi: Tata McGraw-Hill; 2007.
2. Kundur P. Power system stability and control; 8th reprint. New Delhi: Tata McGraw-Hill; 2009.
3. Bevrani H. Robust power system frequency control. New York: Springer; 2009.
4. D.P. Kothari, I.J. Nagrath, Modern power system analysis. 4th ed. New Delhi: Tata McGraw-Hill; 2011.
5. S. Padhan, R.K. Sahu, S. Panda, Automatic generation control with thyristor controlled series compensator including superconducting magnetic energy storage units, Ain Shams Engineering Journal (2014) 5, 759-774.
6. Elgerd OI, Fosha CE. Optimal megawatt-frequency control of multi-area electrical energy systems. IEEE Trans PAS 1970; 89(4):556-63.
7. Daneshfar, F., Bevrani, H., & Mansoori, F. "Bayesian networks design of load-frequency control based on GA". The 2nd International Conference on Control, Instrumentation and Automation, 2011.
8. Ali ES, Abd-Elazim SM. Bacteria foraging optimization algorithm based load frequency controller for interconnected power system. Electr Power Energy Syst 2011; 33:633-8.
9. J. Kennedy, R.C. Eberhart, et al., "Particle Swarm Optimization", In proceedings of IEEE international conference on neural networks, volume 4, pages 1942-1948. Perth, Australia, 1995.
10. K.R. Padiyar., HVDC power transmission systems, New Academic Science, 2011.
11. S. Chaine, M. Tripathy, Design of an optimal SMES for automatic generation control of two area thermal power system using Cuckoo search algorithm, Journal of Electrical and information technology, 2015.
12. M. Farahani, S. Ganjefar, solving LFC problem in an interconnected power system using superconducting magnetic energy storage, Physica C 487 (2013) 60-66.
13. J.C. Bansal, P.K. Singh, Mukesh Saraswat, "Inertia Weight Strategies in Particle Swarm Optimization", 978-1-4577-1123-7/11/\$26.00_c 2011 IEEE.
14. Rout UK, Sahu RK, Panda S. Design and analysis of differential evolution algorithm based automatic generation control for interconnected power system. Ain Shams Eng J 2013; 4(3):409-21.
15. Mohanty B, Panda S, Hota PK. Hybrid BFOA-PSO algorithm for automatic generation control of linear and non-linear interconnected power systems. Appl Soft Comput 2013; 13: 4718-30.

AUTHORS PROFILE



I. Kameswari, student of Mtech in Power system and automation, JNTU Kakinada University, in SRKR Engineering College (A), Bhimavaram, Andhra Pradesh, India. She received Btech Degree from JNTU Kakinada University, Andhra Pradesh, India in 2017. Her research interests include power system, optimization techniques and power quality.



G. Pavan Kumar working as Assistant Professor in SRKR Engineering college (A), Bhimavaram, A.P., INDIA having 14 years teaching experience. He received B.Tech degree from Acharya Nagarjuna University in 2003 and M.Tech degree from JNTU, Anantapur in Feb, 2006. He published about 20 research papers in various conferences and journals.

He is currently pursuing Ph.D in Andhra University.